

Effect of neoclassical poloidal viscosity and resonant magnetic perturbation on the response of the $m/n=1/1$ magnetic island in LHD



B. Huang¹ , S. Satake² , R. Kanno² , Y. Narushima²,
S. Sakakibara², S. Ohdachi², and LHD experiment group

¹The Graduate University for Advanced Studies[SOKENDAI]

²National Institute for Fusion Science

Plasma conference 2014, Nov, 18-21, 2014

- 1 Abstract
- 2 The Motivation of this work
- 3 Simulation with FORTEC-3D
- 4 Simulation Results
 - Radial Profile of NPV and E_r
- 5 Simulation Results
 - Radial Profile of NPV and E_r
 - NPV density dependence on R-axis (@ $\iota \simeq 1$ surface)
 - Dependence of NPV on E_r and Collisionality
- 6 Simulation Results with RMP
 - NPV density on R-axis
 - Dependence of NPV (each (m,n) mode)
- 7 Conclusion and Future work

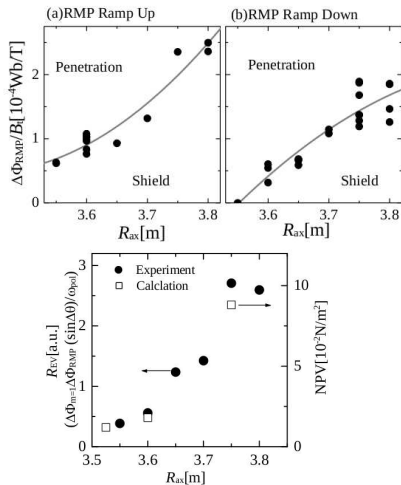
We employ FORTEC-3D to investigate the dependence of neoclassical poloidal viscosity (NPV) on magnetic configuration of LHD, and the effect of resonant magnetic perturbation (RMP) on NPV.

For the $m/n = 1/1$ island formation in LHD, the threshold of RMP amplitude depends on the magnetic axis position in LHD. On the other hand, neoclassical transport theory predicts that the NPV also correlates to the magnetic axis position.

By δf simulation, we investigate NPV variation in LHD plasmas with plasma profiles and ambipolar electric field E_r .

Thus, we study $m/n=1/1$ RMP effect on NPV.

RMP penetrates plasma as its amplitude exceeds the threshold.



- $m/n = 1/1$ RMP in LHD
 - ① RMP penetrate plasma as perturbation amplitude exceeds **threshold**.
 - ② The threshold correlates to **magnetic axis position**.
 - ③ The Neoclassical Poloidal viscosity (**NPV**) also depends on **magnetic axis position**.
- With LHD experiment data (temperature, density, R_{ax}), we investigate the basic dependence of NPV in LHD.

Simulate NPV with FORTEC-3D

We employ drift-kinetic equation for distribution function

$$\delta f(\mathbf{x}, \mathbf{v}) \equiv f(\mathbf{x}, \mathbf{v}) - f_m(\mathbf{x}, \mathbf{v})$$

$$\frac{\partial \delta f}{\partial t} + (\mathbf{v}_{\parallel} + \mathbf{v}_D) \cdot \nabla \delta f + \dot{v} \frac{\partial f}{\partial v} - C_T(\delta f) = -(\mathbf{v}_D \cdot \nabla + \dot{v} \frac{\partial}{\partial v}) f_m + \mathcal{P} f_m. \quad (1)$$

Taking the moment of (1)

$$\left\langle \frac{\partial}{\partial t} m n \mathbf{u} \cdot \mathbf{e}_{\theta} \right\rangle = -\langle \mathbf{e}_{\theta} \cdot \nabla \cdot \mathbf{P} \rangle + e \langle n \mathbf{u} \cdot \nabla \Phi \rangle \quad (2)$$

NPV is defined as

$$\langle \mathbf{e}_{\theta} \cdot \nabla \cdot \mathbf{P} \rangle \equiv \left\langle \frac{\partial \delta P}{B} \frac{\partial B}{\partial \theta} \right\rangle. \quad (3)$$

FORTEC-3D simulates drift kinetic Eq. and evaluate the δP

$$\begin{aligned} \delta P &= \delta P_{\perp} + \delta P_{\parallel} \\ \delta P_{\perp} &= \int d^3 v \frac{m}{2} v_{\perp}^2 \delta f, \quad \delta P_{\parallel} = \int d^3 v m v_{\parallel}^2 \delta f \end{aligned}$$

We scan the magnetic axis from $3.55[m]$ to $3.80[m]$ for ramped-up/down RMP experiments respectively as we show in the fig.(1). In the fig.(2) We investigate NPV amplitude and E_r radial profiles without RMP.

We simulate the ambipolar radial electric field E_r on flux surface by using Γ_i (from FORTEC-3D) and Γ_e (from GSRAKE[4]).

For the investigation of NPV without RMP effect, we collect the data when RMP was shielded.

Simulation Results

Scan the magnet axis from 3.55[m] to 3.8[m] by FORTEC-3D

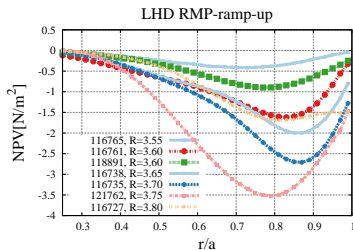


fig.(2a) Radial profile of NPV in ramp-up cases

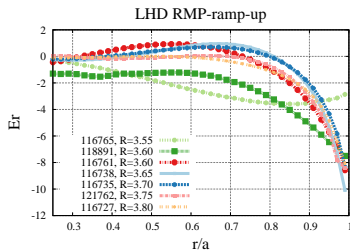


fig.(2b) Radial profile of E_r in ramp-up cases

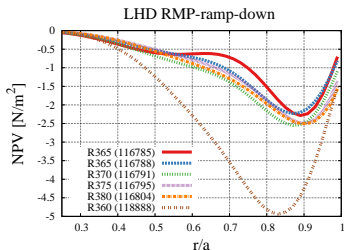


fig.(2c) Radial profile of NPV in ramp-down cases

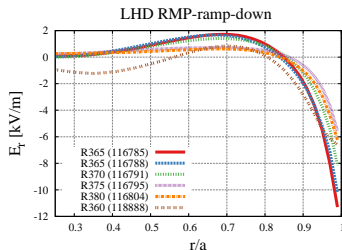


fig.(2d) Radial profile of E_r in ramp-down cases

Simulation Results

NPV density depends on E_r (@ $\iota \simeq 1$ surface)

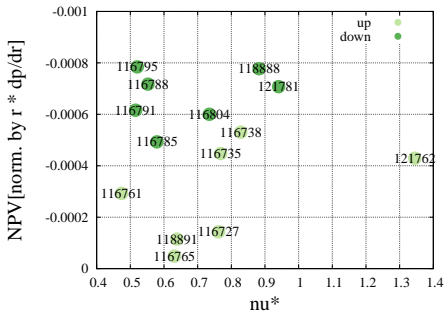


Figure 3: ν_* -NPV.

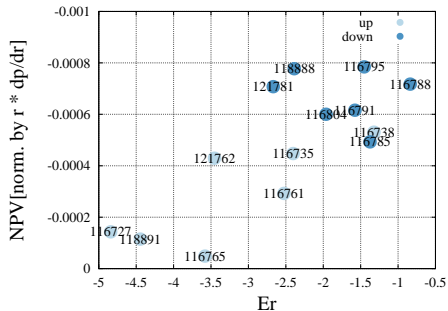


Figure 4: Dependence of NPV on E_r

Simulation Results

NPV depends on R_{ax} but Collisionality

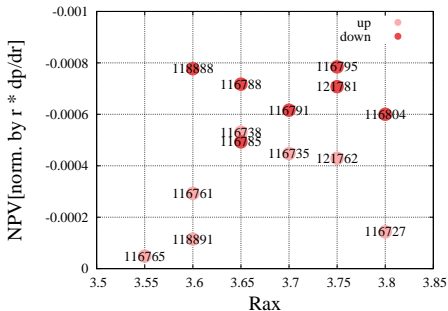


Figure 5: Dependence of NPV on R_{ax}

- We expected that $NPV \propto \frac{1}{nu^*}$, but in fig.(3), the collisionality is not the major factor dominating the amplitude of NPV.
- As neoclassical theory expected, the fig.(4) shows that the NPV amplitude is proportional to $1/|E_r|$.
- In the fig.(5), NPV increases as R_{ax} increases but it is still determined by plasma profile, too. For example, density and ion temperature may be the potential factor. For shot#116727, NPV amplitude decreases due to large E_r amplitude. For shot#11888, NPV is increased but E_r amplitude is small.

Simulation Results with RMP

NPV density on R-axis

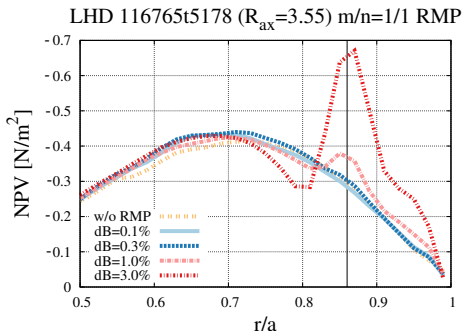


Figure 6: Radial profile of NPV with RMP in a case $R_{ax} = 3.55$

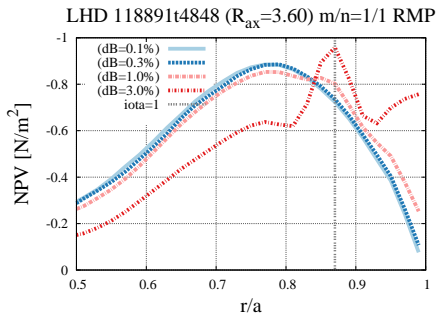


Figure 7: Radial profile of NPV with RMP in a case $R_{ax} = 3.60$

Simulation Results with RMP

NPV density on R-axis

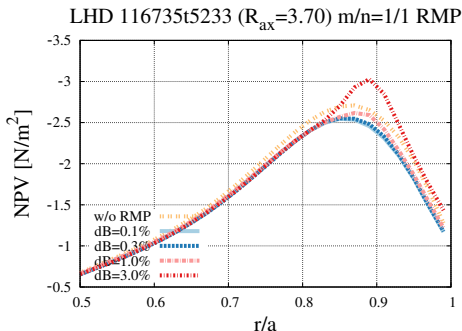


Figure 8: Radial profile of NPV with RMP in a case $R_{ax} = 3.70$

- In figs.(6), (7) and (8), we investigate the NPV with different $m/n=1/1$ RMP amplitude using a simple model $\delta B \propto (r/a)^2$.
- The RMP effect is obvious near $m/n=1/1$ surface.
- We found that below 1% $\delta B/B_0$ amplitude, NPV in LHD is almost unaffected by the RMP field.

Simulation Results

Dependence of NPV (each (m,n) mode)

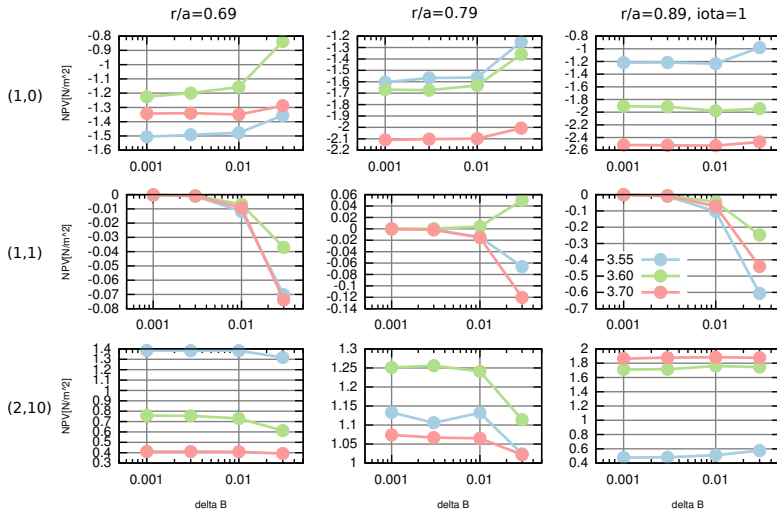


Figure 9: Dependence of NPV at $B(1,0)$, $B(1,1)$ and $B(2,10)$ mode

Simulation Results

Dependence of NPV (each (m,n) mode)

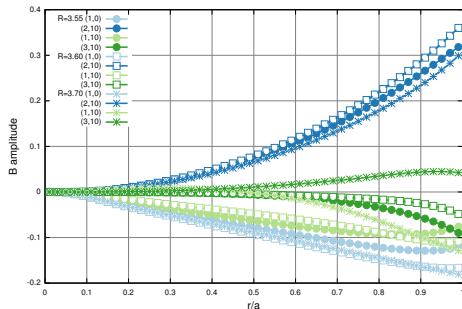


Figure 10: $B_{m,n}$ amplitudes in $R_{ax} = 3.70$, $R_{ax} = 3.65$ and $R_{ax} = 3.55$.

- In fig.10, $B_{1,0}$ and $B_{2,10}$ are main components. The tow components are changed a little due to the shift in R_{ax} . By contrast, $B_{1,10}$ and $B_{3,10}$ are minor but changed a lot due to the shift in R_{ax} .
- In fig.11, $NPV_{1,0}$ and $NPV_{2,10}$ sum is small to contribute to total NVP too much. In Fig.12, $NPV_{1,10}$ and $NPV_{3,10}$ sum is main contribution for NPV.

Simulation Results

Dependence of NPV (each (m,n) mode)

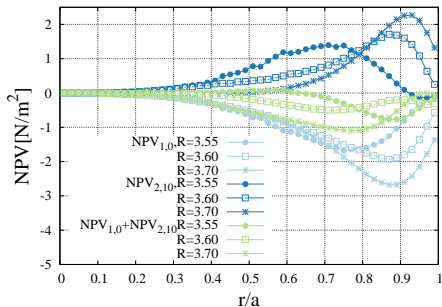


Figure 11: NPV contribution of B(1,0) and B(2,10) without RMP in $R_{ax} = 3.70$, $R_{ax} = 3.65$ and $R_{ax} = 3.55$.

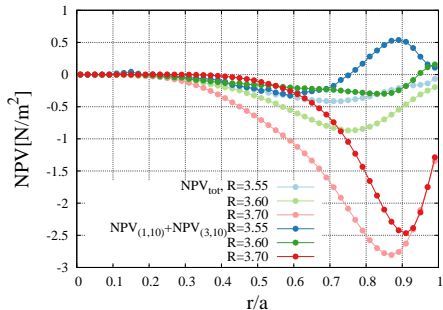


Figure 12: NPV contribution of B(1,10) and B(3,10) without RMP in $R_{ax} = 3.70$, $R_{ax} = 3.65$ and $R_{ax} = 3.55$.

Dependence of NPV (each (m,n) mode)

We construct the NPV by

$$\langle \mathbf{e}_\theta \cdot \nabla \cdot \mathbf{P} \rangle = \sum_{m,n \neq 0} \langle \mathbf{e}_\theta \cdot \nabla \cdot \mathbf{P} \rangle_{m,n} \equiv B_0 \sum_{m,n \neq 0} n \delta_{m,n} Q_{m,n}. \quad (4)$$

- 1 As expected, the RMP, mode $B(1,1)$, affects surface $\iota \simeq 1$ and the effect is proportional to RMP amplitude.
- 2 In the other surface ($r/a=0.69$ and 0.79), it is small and negligible to the RMP effect on mode $B(1,1)$. The strong RMP influences the $(1,0)$ - and $(2,10)$ - modes and changes their amplitudes. This suggests that the strong RMP $\delta B_{m,n}$ couple with the pressure perturbation of the different modes, $Q_{m',n'}$.
- 3 Practically $\delta B/B_0 \sim 10^{-4}$ in LHD but we employ $\delta B/B_0 \sim 10^{-2}$ in our test. It is anticipated that the RMP field does not change NPV amplitude in the practical LHD experiment.

- Conclusion

- NPV amplitude becomes larger as R_{ax} moves outward. Following the results, we are able to see the influence near the resonant surface ($\nu \simeq 1$) if the RMP amplitude $\delta B/B_0 > 0.01$. Practically RMP amplitude is $\delta B/B_0 \sim 10^{-4}$ in LHD. We found that $m/n = 1/1$ RMP less than 1% cannot affect NPV.
- The strong RMP influences the mode $B(1, 0)$ and $B(2, 10)$ and changes their amplitudes.

- Future work

- Study the relation between the NPV torque with the threshold RMP amplitude from the LHD experiments.
- Compare the E_r profile obtained from the ambipolar condition with the measured.

Referece

- [1] Sakakibara,et al.,(2013). In Nuclear Fusion 53, p. 043010.
- [2] Narushima, Y.,et al.,(2011). In Nuclear Fusion 51, p. 083030.
- [3] Satake, S.,et al.(2011). In Plasma Physics and Controlled Fusion 53, p. 054018.
- [4] C D Beidler and W D D'haeseleer (1995) Plasma Phys. Control. Fusion 37 463

Acknowledgment

This work is pported by NIFS collaborative Research Programs NIFS13KNST051, and JSPS Grant-in-Aid for Young Scientists (B), No. 23760810. Part of calculations was carried out using the HELIOS supercomputer at IFERC-CSC, under the ITER-BA collaboration implemented by Fusion for Energy and JAEA. This presentation received the "financial support program for international conference presentations provided by the Course-by-Course Education Program of SOKENDAI.